U. S. Department
of Transportation

**Federal Railroad
Administration**

Office of Research
and Development
Washington, DC 20590

Evaluation of Railroad Cab Car End Beam Designs

Rail Passenger Equipment Collision Tests

ck-Train Dynamics

REPORT DOCUMENTATION PAGE

1. AGENCY USE ONLY (Leave blank)	2. REPORT DATE June 2003	3. REPORT TYPE AND DATES COVERED Final Report

4. TITLE AND SUBTITLE
Evaluation of Railroad Cab Car End Beam Designs

5. FUNDING NUMBERS
RR-128/R1001

6. AUTHOR(S)
Ronald A. Mayville, Randolph P. Hammond, Kent N. Johnson

7. PERFORMING ORGANIZATION NAME(S) AND ADDRESS(ES)
Arthur D. Little, Inc. *
Acorn Park
Cambridge, MA 02140-2390

8. PERFORMING ORGANIZATION REPORT NUMBER
DOT-VNTSC-FRA-03-05

9. SPONSORING/MONITORING AGENCY NAME(S) AND ADDRESS(ES)
U. S. Department of Transportation
Federal Railroad Administration
Office of Research and Development
1120 Vermont Avenue, NW
Mail Stop 20
Washington, DC 20590

10. SPONSORING/MONITORING AGENCY REPORT NUMBER
DOT/FRA/ORD-02/08

11. SUPPLEMENTARY NOTES
*Under contract to:
U.S. Department of Transportation
Research and Special Programs Administration
John A. Volpe National Transportation Systems Center
Cambridge, MA 02142-1093

12a. DISTRIBUTION/AVAILABILITY STATEMENT
This document is available to the U.S. public through the National Technical Information Service, Springfield VA 22161. This document is also available on the FRA web site at www.fra.dot.gov.

12b. DISTRIBUTION CODE

13. ABSTRACT (Maximum 200 words)

This report presents the results of an experimental study to establish the strength and energy absorption capability of railroad cab car corner structures built to current requirements and for structures modified to carry higher loads and absorb more energy. Current cab car structures were reviewed and an end beam test element was designed with a corner post support baseline strength of at least 150,000 lbf. This design was modified to provide a strength of over 400,000 lbf. Three tests were conducted, one static and two dynamic. All experiments were accompanied by nonlinear, dynamic finite element analysis. It was observed that the strength of the baseline element was 30 percent greater than the design value and that approximately 100kJ of energy was absorbed before fracture. Static and dynamic analyses and test results agreed quite closely. The drop tower test conducted with an end beam test article that had been reinforced with a column had a peak load greater than 400,000 lbf. The energy absorption capability of the modified system was over four times that of the baseline configuration. These results demonstrate that significant improvement can be made to cab car corner structures with relatively minor modifications to current design.

14. SUBJECT TERMS
Cab car end beam, finite element analysis, static and dynamic tests, drop tower test, quasi-static loading, crashworthiness, baseline test article, side sill, railroad

15. NUMBER OF PAGES
50

16. PRICE CODE

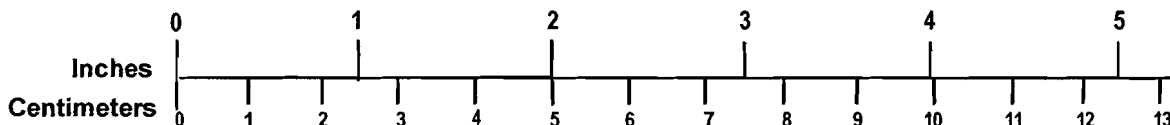| 17. SECURITY CLASSIFICATION OF REPORT	18. SECURITY CLASSIFICATION OF THIS PAGE	19. SECURITY CLASSIFICATION OF ABSTRACT	20. LIMITATION OF ABSTRACT
Unclassified	Unclassified	Unclassified	Unlimited
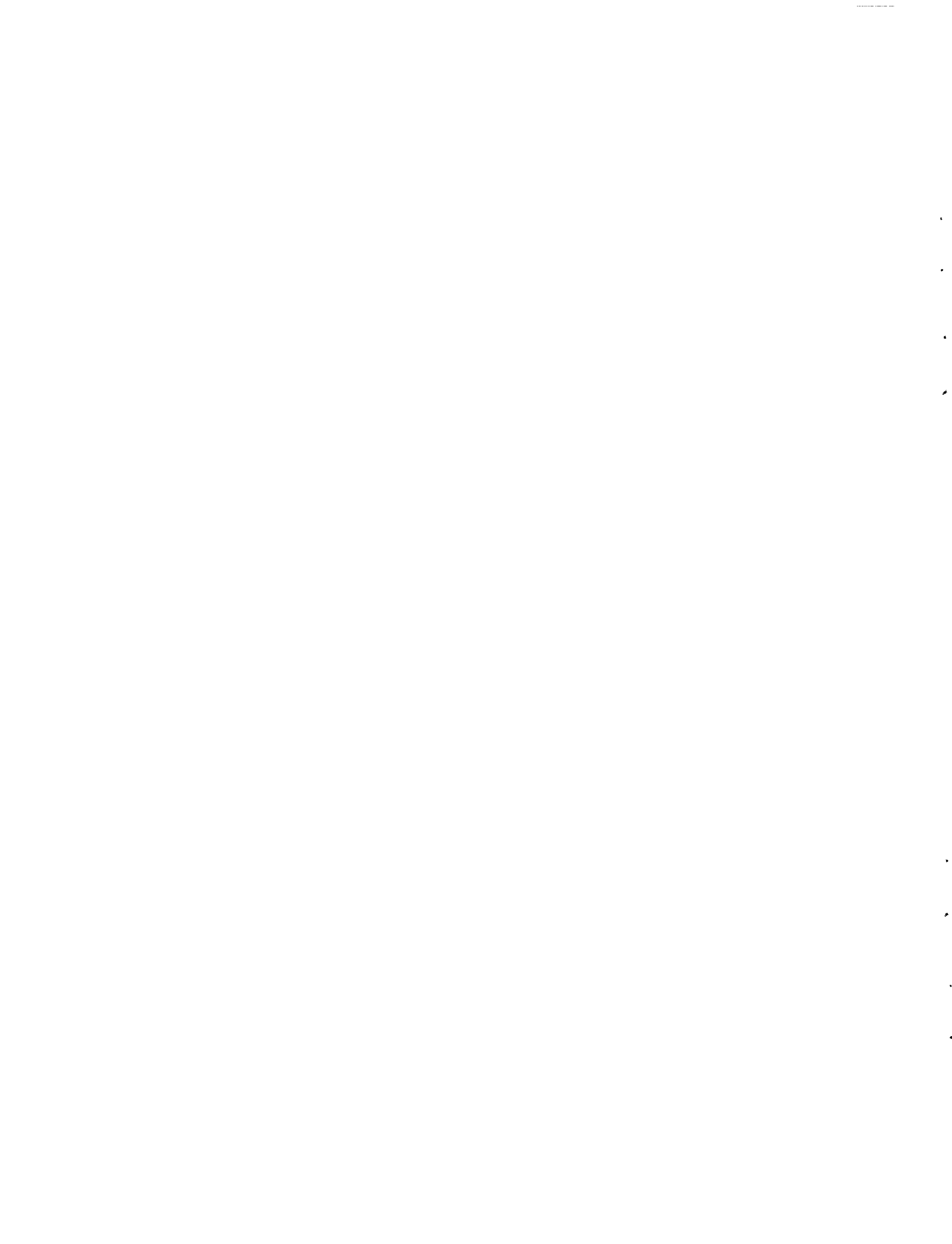
METRIC/ENGLISH CONVERSION FACTORS

ENGLISH TO METRIC

METRIC TO ENGLISH

LENGTH (APPROXIMATE)

1 inch (in)	= 2.5 centimeters (cm)
1 foot (ft)	= 30 centimeters (cm)
1 yard (yd)	= 0.9 meter (m)
1 mile (mi)	= 1.6 kilometers (km)

LENGTH (APPROXIMATE)

1 millimeter (mm)	= 0.04 inch (in)
1 centimeter (cm)	= 0.4 inch (in)
1 meter (m)	= 3.3 feet (ft)
1 meter (m)	= 1.1 yards (yd)
1 kilometer (km)	= 0.6 mile (mi)

AREA (APPROXIMATE)

1 square inch (sq in, in^2)	= 6.5 square centimeters (cm^2)
1 square foot (sq ft, ft^2)	= 0.09 square meter (m^2)
1 square yard (sq yd, yd^2)	= 0.8 square meter (m^2)
1 square mile (sq mi, mi^2)	= 2.6 square kilometers (km^2)
1 acre = 0.4 hectare (he)	= 4,000 square meters (m^2)

AREA (APPROXIMATE)

1 square centimeter (cm^2)	= 0.16 square inch (sq in, in^2)
1 square meter (m^2)	= 1.2 square yards (sq yd, yd^2)
1 square kilometer (km^2)	= 0.4 square mile (sq mi, mi^2)
10,000 square meters (m^2)	= 1 hectare (ha) = 2.5 acres

MASS - WEIGHT (APPROXIMATE)

1 ounce (oz)	= 28 grams (gm)
1 pound (lb)	= 0.45 kilogram (kg)
1 short ton = 2,000 pounds (lb)	= 0.9 tonne (t)

MASS - WEIGHT (APPROXIMATE)

1 gram (gm)	= 0.036 ounce (oz)
1 kilogram (kg)	= 2.2 pounds (lb)
1 tonne (t)	= 1,000 kilograms (kg)
	= 1.1 short tons

VOLUME (APPROXIMATE)

1 teaspoon (tsp)	= 5 milliliters (ml)
1 tablespoon (tbsp)	= 15 milliliters (ml)
1 fluid ounce (fl oz)	= 30 milliliters (ml)
1 cup (c)	= 0.24 liter (l)
1 pint (pt)	= 0.47 liter (l)
1 quart (qt)	= 0.96 liter (l)
1 gallon (gal)	= 3.8 liters (l)
1 cubic foot (cu ft, ft^3)	= 0.03 cubic meter (m^3)
1 cubic yard (cu yd, yd^3)	= 0.76 cubic meter (m^3)

VOLUME (APPROXIMATE)

1 milliliter (ml)	= 0.03 fluid ounce (fl oz)
1 liter (l)	= 2.1 pints (pt)
1 liter (l)	= 1.06 quarts (qt)
1 liter (l)	= 0.26 gallon (gal)
1 cubic meter (m^3)	= 36 cubic feet (cu ft, ft^3)
1 cubic meter (m^3)	= 1.3 cubic yards (cu yd, yd^3)

TEMPERATURE (EXACT)

$[(x-32)(5/9)]$ °F = y °C

TEMPERATURE (EXACT)

$[(9/5) y + 32]$ °C = x °F

QUICK INCH - CENTIMETER LENGTH CONVERSION

Inches	0	1	2	3	4	5

Centimeters	0	1	2	3	4	5	6	7	8	9	10	11	12	13

QUICK FAHRENHEIT - CELSIUS TEMPERATURE CONVERSION

°F	-40°	-22°	-4°	14°	32°	50°	68°	86°	104°	122°	140°	158°	176°	194°	212°
°C	-40°	-30°	-20°	-10°	0°	10°	20°	30°	40°	50°	60°	70°	80°	90°	100°
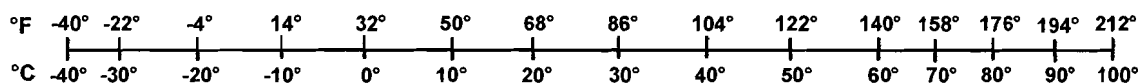
For more exact and or other conversion factors, see NIST Miscellaneous Publication 286, Units of Weights and Measures. Price $2.50 SD Catalog No. C13 10286
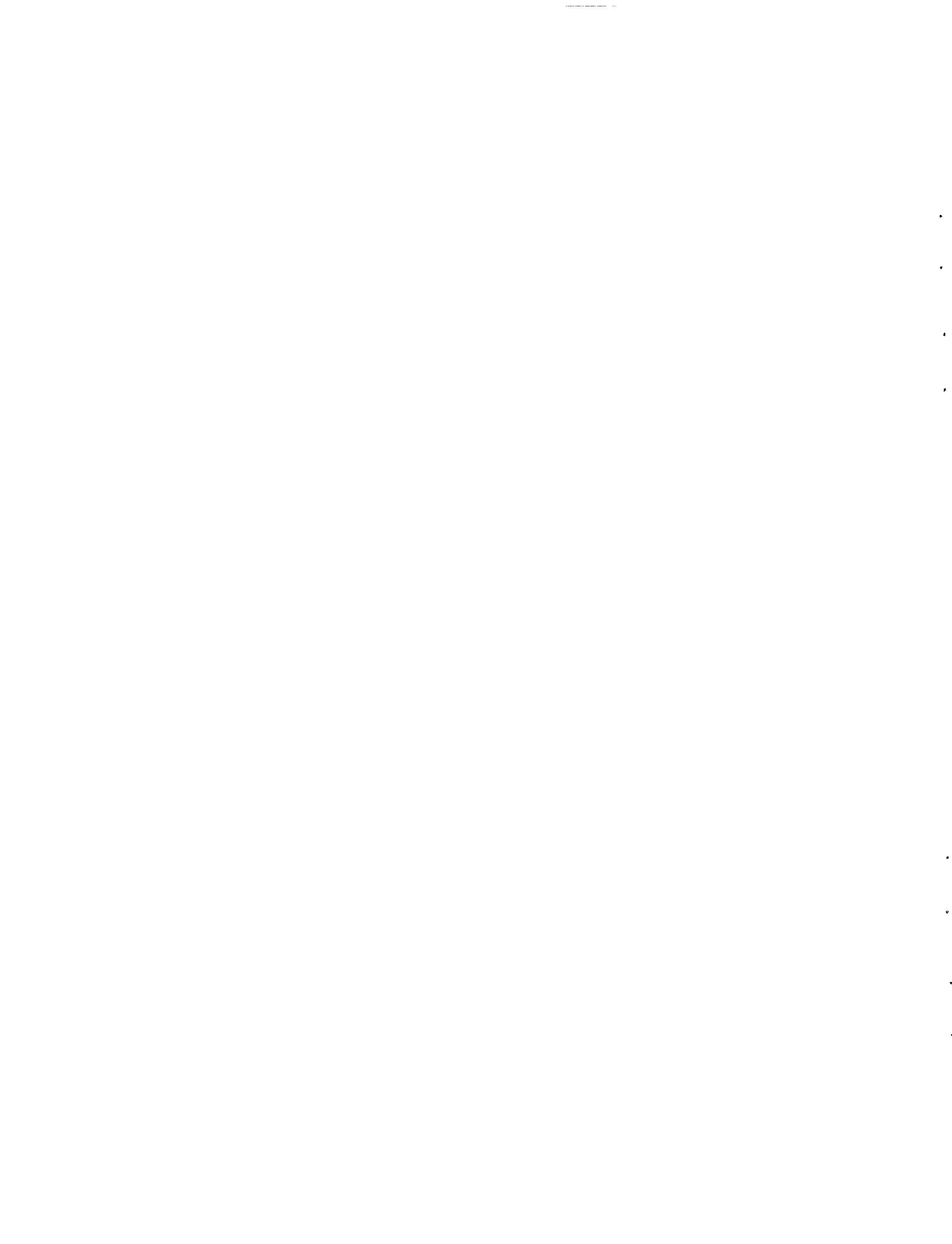
Updated 6/17/98

TABLE OF CONTENTS

LIST OF FIGURES

LIST OF TABLES

EXECUTIVE SUMMARY

A number of train accidents over the last few years have demonstrated that the corner of cab cars can be subjected to impacts that endanger crew and passengers. Recent research conducted under the direction of the Volpe National Transportation Systems Center (Volpe Center) for the Federal Railroad Administration (FRA) has shown that cab car operator's volume can be crushed in speeds as low as 15 mph for an offset collision with another train.

Analyses have, however, also demonstrated that the crashworthiness of cab cars subjected to offset collisions can be substantially improved with relatively modest modifications. These studies have shown that the collision speed at which protection is provided to the operator can be increased by about 50 percent by ensuring that the corner structure can sustain a load of 300,000 lbf for a limited amount of crush. The higher strength can be achieved by bringing the side sill forward to the corner post base. The added strength and energy absorption provided by this and other types of modifications are now being considered by the railroad industry.

This report presents the results of an experimental study to establish the strength and energy absorption capability of cab car corner structures built to current requirements and for structures modified to carry higher loads and absorb more energy.

This project included the design, fabrication, analysis, and testing of cab car corner end beam structural elements, with two strength levels. In one case, the structural element was intended to have a geometry and strength typical of that used in cab cars built to current structural specifications. In the second case, this structural element was modified to achieve a substantially higher strength with the possibility of much greater energy absorption capability. The modification was made in a way that would be relatively easy to implement in new vehicle construction.

With a few exceptions, high-strength, low-alloy steel was used for the plate components of the end beam test article and fixture. This steel meets the standard specification of ASTM A572 Grade 50 steel. The baseline test article was designed to have a corner post support strength of 150,000 lbf, using conventional structural engineering techniques. This design was then modified to provide a strength of over 400,000 lbf.

Three tests were conducted, one static and two dynamic tests. The testing included quasi-static loading of one of the baseline test articles to ensure that it met the ultimate strength of 150,000 lbf, and dynamic drop tower testing of a baseline and modified test article to measure the energy absorption capacity. The experiments were accompanied by nonlinear, dynamic, finite element analysis. The drop tower test conducted with an end beam test article that had been reinforced with a column had a peak load greater than 400,000 lbf, and the energy absorption capability of the modified system was over four times that of the baseline configuration.

The dynamic test results verify that higher strength and energy absorption of the corners of cab cars can be achieved with the addition of the side sill member and that the nonlinear finite element analysis provides good predictions of the response, provided that accurate material data are used.

1.   INTRODUCTION

A number of train accidents over the last few years and recent research conducted under the direction of the Volpe Center have demonstrated that the corner of cab cars can be subjected to impacts that endanger crew and passengers. Figure 1 shows a photograph of the cab car struck by a locomotive at a switch in Secaucus, New Jersey, in 1996 [1]. Other accidents have included Silver Spring, Maryland, also in 1996 [2], and Gary, Indiana in 1993 [3].

Figure 1.   Photograph of the Cab Car Damaged in the Secaucus, New Jersey, Accident

Finite element analyses have shown [4,5] that a collision speed as low as 15 mph could crush the cab car operator's volume for an offset collision with another train.

However, analyses have also demonstrated that the crashworthiness of cab cars subjected to offset collisions can be substantially improved with relatively modest increases in performance requirements. In particular, these studies have shown that the collision speed at which protection is provided to the operator can be increased by about 50 percent by ensuring that the corner structure can achieve a maximum load of 300,000 lbf for limited amounts of crush. This higher strength can be achieved by bringing the side sill forward to the corner post base. The added strength and energy absorption provided by this and other types of modifications are now being considered by the rail industry.

This project was carried out to experimentally investigate the strength and energy absorption provided by cab car corner structures built to current industry standards and those that are modified to possess higher strengths with some energy absorption capability.

The results verify that substantially greater strength and energy absorption can be achieved with the addition of the side sill member and that the nonlinear finite element analysis provides good predictions of the response, provided accurate material data are used.

The approach to this project included design, fabrication, analysis, and testing of cab car corner end beam structural elements, with two strength levels. In one case, the structural element was intended to have a typical geometry and strength of that used in cab cars built to current structural specifications. In the second case, this structural element was modified to achieve a substantially higher strength with the possibility of much greater energy absorption capability. In particular, the modification was made in a way that would be relatively easy to implement in new vehicle construction. Table 1 lists the tests conducted and the target end beam strengths.

Table 1. End Beam Tests Conducted

Test	Target End Beam Strength	Loading Method
1	150,000 lbf	Quasi-Static
2	150,000 lbf	Dynamic
3	400,000 lbf	Dynamic

The first test was conducted under quasi-static loading, since the corners of cab cars are currently designed under this assumption. It was also necessary to have test results for which the loading characteristics were accurately known so that good comparisons could be made to the companion finite element analysis.

The tasks undertaken in this program included a review of current cab car corner construction, design and fabrication of test articles and test fixtures, hand calculations, and finite element analysis of the test articles and fixture, and actual testing.

2.   REVIEW OF CAB CAR CORNER CONSTRUCTION

The strength requirements and construction types for the corners of a number of cab cars currently in operation in the U.S. were reviewed before the detailed design of the test article was generated. While there were, at the time of this project, no federal requirements for corner strength, industry practice required that the corner post have an ultimate strength of 150,000 lbf applied at the base along the axis of the car. The strict interpretation of this requirement is that only the corner post itself and any reinforcement used need to possess the shear strength; the structure to which the post is attached need not. However, it is understood that both the support structure and the post itself are generally designed to carry the 150,000-lbf load without failure. The corner post is also usually required to carry a load of about 30,000 lbf applied 18 in. above the floor, without causing material yield.

In general, it was found that cab cars, like most railroad passenger cars operated in commuter or intercity service in the U.S., have an end underframe design similar to that schematically shown in Figure 2. The buff (end compression) load requirement, which for these vehicles is usually 800,000 lbf, is carried by the draft or center sill, which runs down the center of the car. The corner post is usually supported at its base by a cantilever beam called the "end beam" or "buffer wing." This type of construction is used to accommodate the stairwell that is normally located near all four corners of the vehicle. During cab operation, a plate drops down to provide a place to sit for the operator.
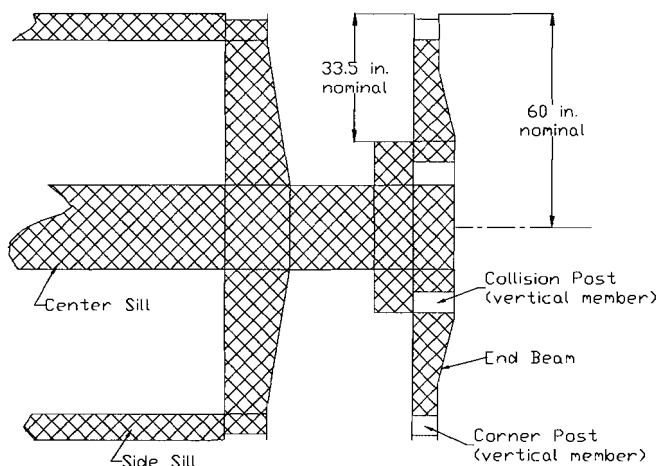
Figure 2. Typical End Underframe Design for Passenger Rail Vehicles Operated in Commuter and Intercity Service in the U.S.

The T-shaped construction shown at the end of the underframe in Figure 2 is sometimes called the buffer sill and it often includes two rectangular holes that are used to anchor the collision posts, which are located on each side of a doorway.

The ends of most U.S. commuter and intercity rail vehicles are constructed from high tensile structural steel having a yield strength of 50ksi, and welded construction is typical in the buffer sill.

3. TEST ARTICLE AND FIXTURE DESIGN

The final design of the test article was achieved from an interactive process in which hand calculations were accompanied by finite element analysis. The final designs appear in this section and the analyses are summarized in Section 6.

Figures 3 and 4 show the final design of the baseline test article and the test fixture used in this program. The test article was designed to meet the following criteria:

- An ultimate strength of 150,000 lbf for a load applied in the longitudinal direction at the center point of the corner post base;
- Dimensions representative of actual U.S. cab cars;
- Materials and welding techniques representative of current U.S. rail car industry practice;
- Easy connection to a test fixture that can be used for both static and dynamic tests; and
- Failure occurring in the part of the end beam meant to represent the vehicle.

The resulting design (Figure 3) represents rail vehicle construction of all parts except the fixture attachment surfaces. The design does not include a corner post because there was more interest in loading on the corner post support structure, such as would occur in a collision with another cab car or a locomotive. However, the design does include a hollow rectangular section at the very end that could accommodate a corner post. The configuration also incorporates a hollow rectangular section in which a collision post could be accommodated. As will be shown, this is the very location at which failure occurs in the tests.

Figure 4 shows a drawing of the test fixture with the baseline test article. The test article is attached to the fixture by means of 16 removable bolts. The fixture is in turn attached by welding (in the quasi-static test) or by bolts (in the drop tower tests) to the "foundation" along the left-hand (vertical) surface shown in Figure 4. The fixture was designed to carry a load, without yield, of 450,000 lbf applied at test article corner post location. The dimensions of Figures 3 and 4 are in inches.

5
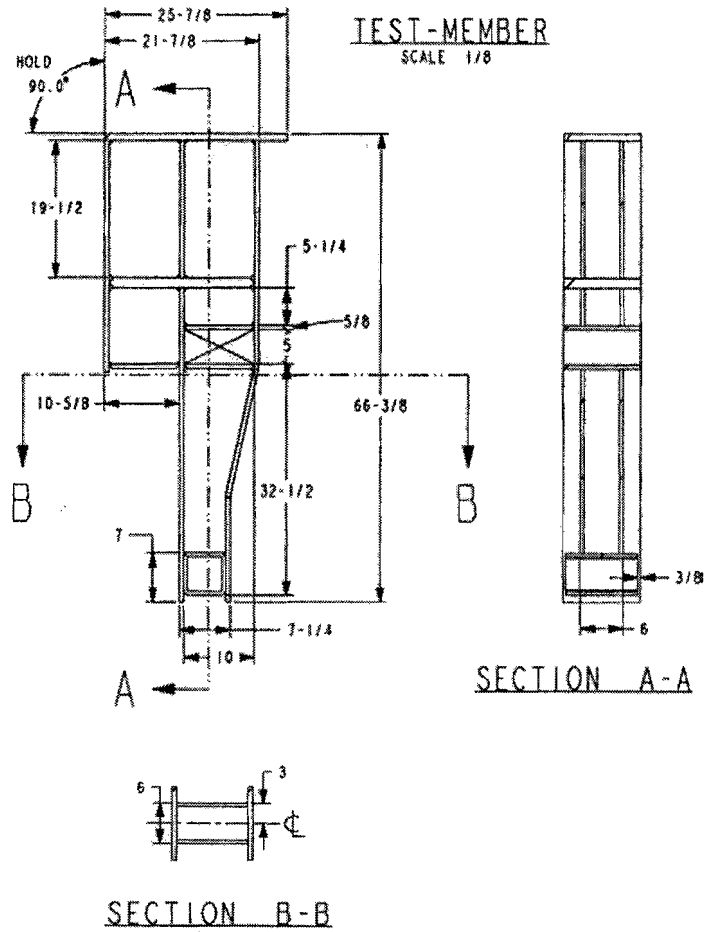
Figure 3. The Mechanical Drawing for the Baseline Test Article
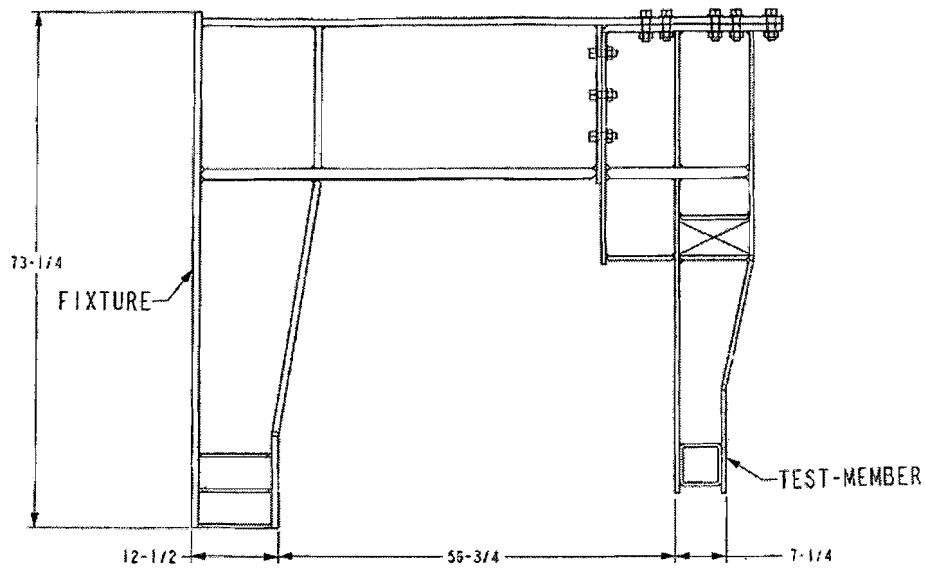
Figure 4. Design of the Test Fixture with the Baseline Test Article Attached

6
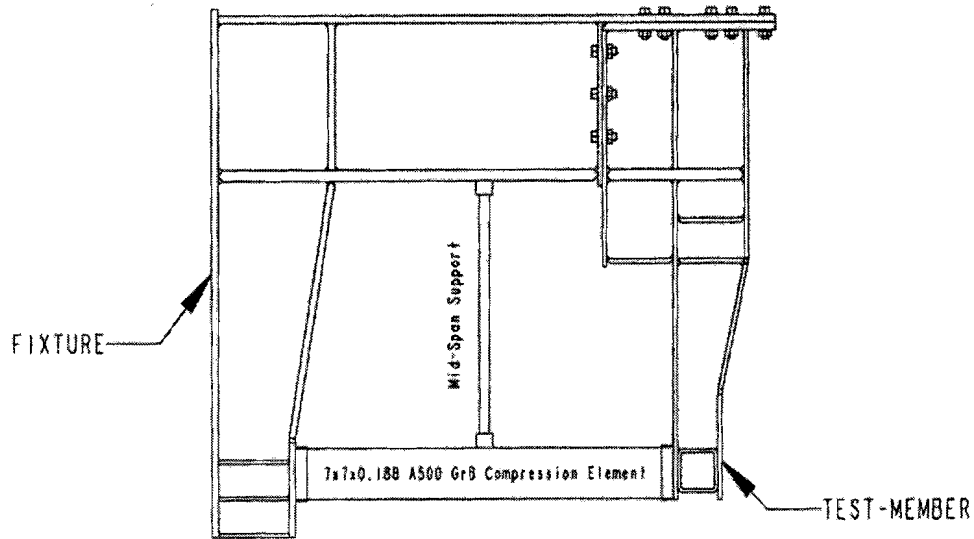
Figure 5. Modified Test Article Design with Fixture

Figure 5 shows the modified test article. A longitudinal member was added between the back of the corner post location and the end of the fixture. This member represents a strengthened side sill brought forward to the corner post. This side sill member was welded to the test article and fixture using tubular lug reinforcements to eliminate the risk of connection fracture. A transverse member was also added to provide lateral support against buckling.

Figure 6 shows the design for the load application fixture for the static test; a similar but solid-block design was used for the drop tower tests. The dimensions of Figure 6 are in inches.
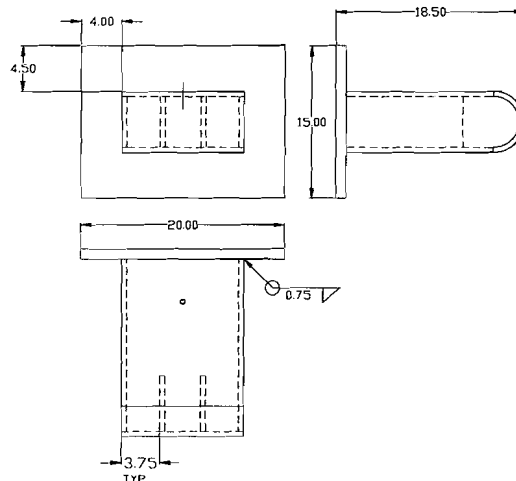
Figure 6. The Design for the Fixture Used to Apply Load to the End Beam Test Article in the Quasi-Static Test

4. MATERIALS AND PROPERTIES

A high strength, low alloy steel was used for the plate components of the end beam test article and fixture, with a few exceptions as noted below. This steel meets the standard specification of ASTM A572 Grade 50 steel. The ASTM standard demands that the yield and ultimate strengths be as shown in Table 2.

Table 2. Required Minimum Properties for ASTM A572 Grade 50 Steel

Minimum Yield Strength (lbf/in.^{2})	Minimum Ultimate Tensile Strength (lbf/in.^{2})
50,000	65,000

ASTM A572 Grade 50 steel is commercially available as INX 50[®] and EX-TEN 50[®]. Along with COR-TEN[®] A (ASTM A242) and COR-TEN[®] B (ASTM A588), the steel finds common application in the rail car industry.

Tensile specimens were machined from excess 0.50-in. thick plate supplied with the end beam/fixture materials. The specimens were machined in accordance with ASTM A370. Three specimens were cut parallel to and three specimens perpendicular to the rolling direction. Average properties from the tests are shown in Table 3.

Table 3. Measured Properties for the ASTM A572 Grade 50 Used to Fabricate the Test Articles and Test Fixture

Coupon Relation to Roll Direction	0.2% Offset Yield Strength (lbf/in.^{2})	Tensile Strength (lbf/in.^{2})	Total Elongation (%)	Reduction of Area (%)
parallel	57,000	78,400	30	70.7
perpendicular	56,800	77,800	27	60.1

The material satisfied ASTM A572 Grade 50.

The 6 in. x 6 in. section used to represent the corner post lug was made from ASTM A500 Grade B tube. The compression element and its mid-span support of the modified end beam were also made from the same material. A500 Grade B has the minimum required properties shown in Table 4. The actual properties of this material were not measured.

Table 4. Required Minimum Properties for ASTM A500 Grade B Steel

Minimum Yield Strength (lbf/in.^{2})	Minimum Ultimate Tensile Strength (lbf/in.^{2})
46,000	58,000

The bolts used to join the test article to the fixture were 1.0 in. diameter, Grade 8 bolts. Sixteen bolts, Grade 8 nuts and hardened washers were used to effect the interface. An installation torque of 890 ft-lbf was used. The attachment was designed to be stronger than the test article, to assure that the attachment response remained elastic, while the test article plastically deformed.

The weld material used to construct the fixture and end beams met AWS A5.18, whose required properties are shown in Table 5.

Table 5. Required Minimum Properties for AWS 5.18 MIG Wire

Minimum Yield Strength (lbf/in.^{2})	Minimum Ultimate Tensile Strength (lbf/in.^{2})
60,000	72,000

The true-stress strain curve was not measured for any of the materials as it was a difficult and expensive test to perform. However, the ADL curve shown in Figure 7 was used. This curve corresponds to a power-law relationship:

$$\sigma = Ae^n,$$

with $A = 150$ and $n = 0.3$ for stress in units of 10^3 lbf/in^2. The value of n = 0.3 is representative of the types of structural steels used to fabricate the test articles. The elastic constants used were, Young's Modulus = 29 x 10^6 lbf/in.^{2} and Poisson's Ratio = 0.29. These properties were used for all of the components in the analyses.
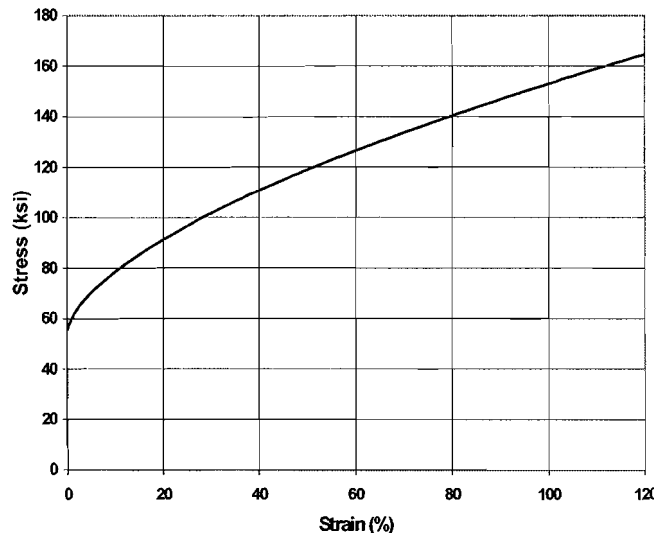
Figure 7. True Stress-Strain Curve Used for the A572 Steel in the Finite Element Analysis

Strain rate effects on the material properties were not considered in this project.

The following fracture criterion was used in the finite element analysis:

$$e_f = \frac{e_t}{3(\frac{\sigma_m}{\sigma_e})},$$

where e_f = strain to fracture under general states of stress

e_t = true strain to fracture in a tension test

σ_m = mean stress (average of the principal stresses)

σ_e = effective or Mises stress.

The true strain to fracture of 1.05 is derived from the tension test and for the A572 material.

11
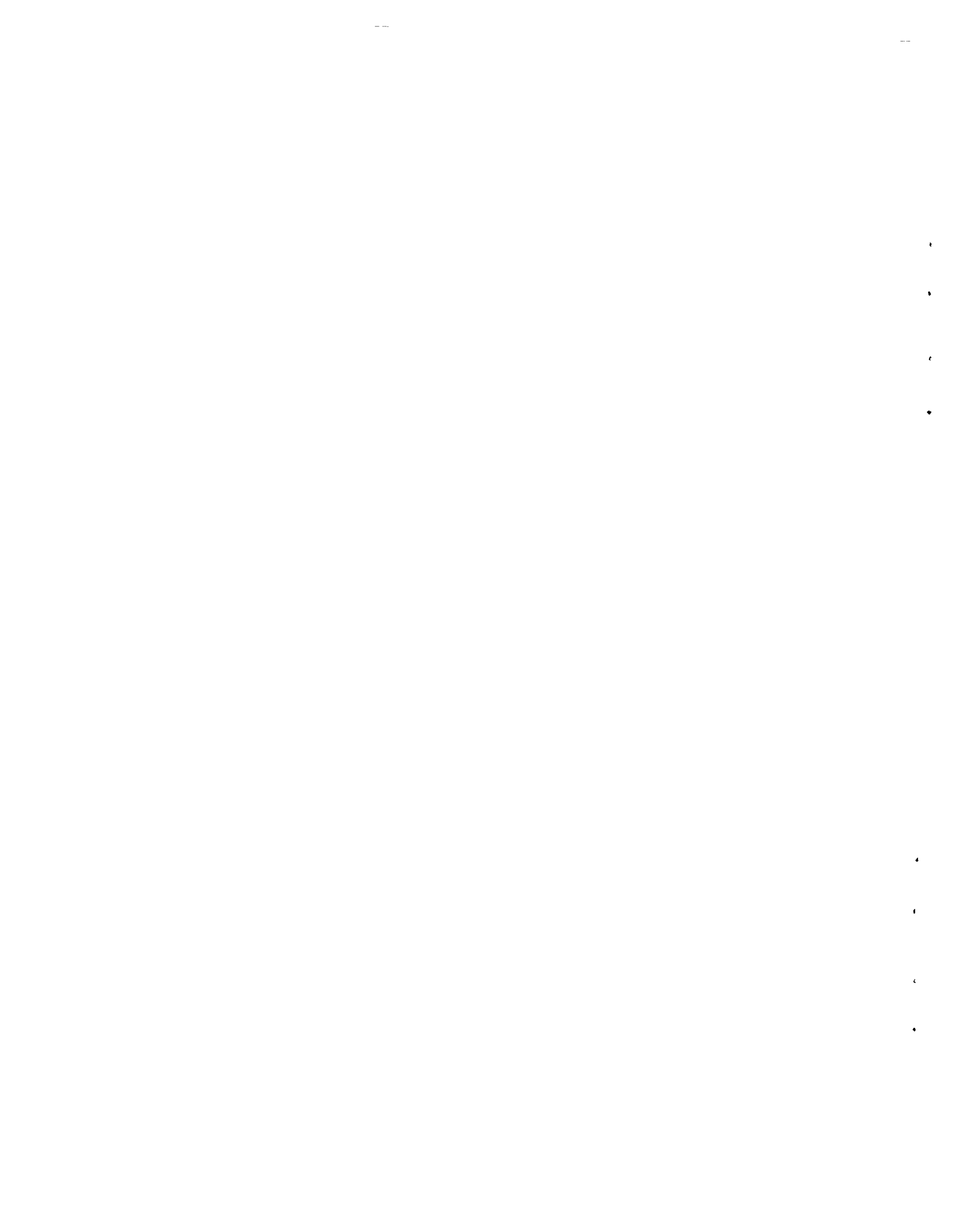
5. ANALYSIS

5.1 BASELINE TEST ARTICLE

The baseline test article was designed to have a corner post support strength of 150,000 lbf using conventional structural engineering techniques. Analysis revealed that the strength of an end beam with the type of design shown in Figure 3 is determined by the strength of the plate element on the front side of the collision post opening. In fact, the ultimate strength for a load applied at the corner post in the longitudinal direction is given approximately by (see Figure 8):

$$F = A(\sigma_{ult})\left(\frac{w}{h}\right)$$

where A = the cross-sectional area of the plate element at the front of the collision post opening

σ_{ult} = the ultimate tensile strength

w = the depth of the end beam at the collision post opening

h = the distance from the collision post opening to the center of the corner post opening.

The exact force will be slightly greater than the force calculation by the equation due to the moment resistance at the hinge point.
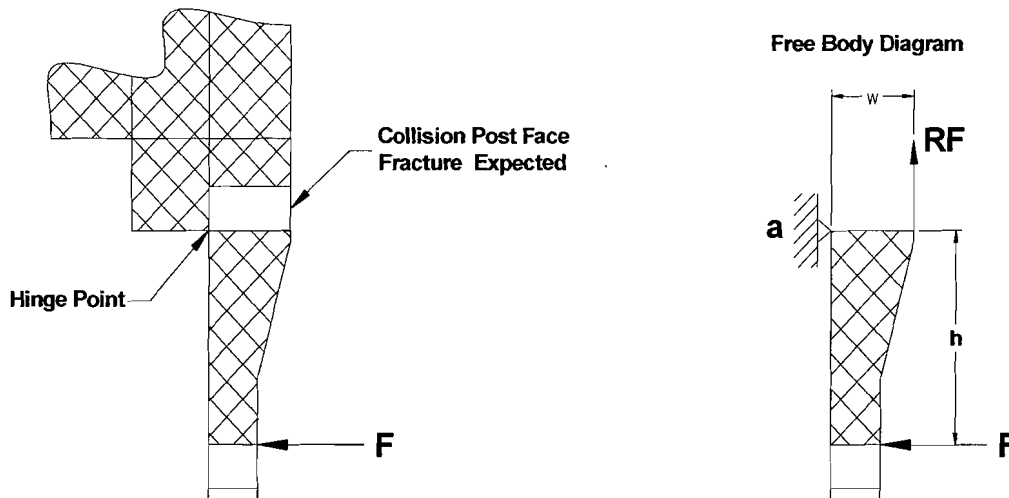
Figure 8. Approximate Force System on the End Beam at Failure

In the design, $A = (0.625)(11.0) = 6.88$ in.^{2}

$\sigma_{ult} = 65,000$ lbf/in.^{2} (specified minimum tensile strength)

$w = 10.6$ in.
$h = 29.4$ in.

Which gives, $F = 161,000$ lbf.

This value is close to and above the required strength value. However, the actual strength is much higher because the measured tensile strength (Table 3) is 78,000 lbf/in.^{2}, 20 percent higher than the value assumed in design. Indeed, as shown in the section on testing, the measured strength was approximately 30 percent higher, demonstrating the conservative nature of the common structural engineering approach used in most rail vehicle ultimate strength designs.

Finite element analysis was conducted for both quasi-static and dynamic loading of the baseline test article to ensure that failure would occur in the components meant to represent the rail vehicle and to ensure that the test fixture would not be deformed or damaged in the static and dynamic tests.

A half-symmetrical finite element model of the baseline end beam and fixture was created using the commercially available ABAQUS® non-linear finite element computer programs (ABAQUS Standard to simulate the quasi-static loading, and ABAQUS Explicit to simulate dynamic loading). A total of 2,578 quad-plate elements and 2,679 nodes comprised the half-symmetrical end beam/fixture model. The undeformed model is presented in Figure 9.

Loading was applied in the static case through a set of rigid elements meant to simulate the loading ram, which had a radius of 3 in. Contact friction was not included. The load was centered at a point of the end beam at the inner edge of the corner post opening (as opposed to the center of the opening as assumed in design). This is the location of load application used in the tests. The rigid loading surface was constrained to follow the original line of loading without other translations or rotations.

A similar contact configuration was simulated in the dynamic analysis. Loading was applied by simulating a rigid mass (4,150 lbm to simulate actual test conditions, 40,000 lbm to obtain the overall load-crush response) traveling at a speed of 29 ft/sec. at impact. This mass was also constrained against all motion except translation along the original path.
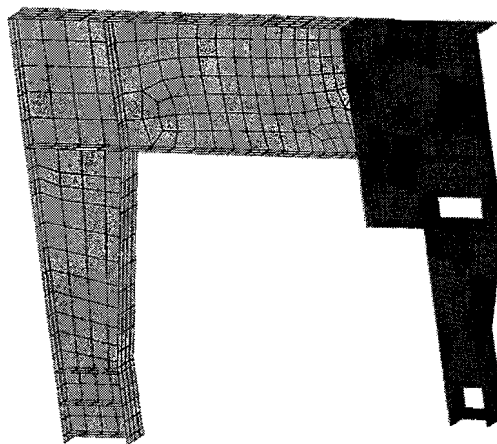

Figure 9. Half-Symmetrical End Beam/Fixture Finite Element Model

Figure 10 shows the load-deformation plot predicted for the baseline end beam configuration for both quasi-static and dynamic loading. Both analyses provide an end beam strength close to 240,000 lbf. This value is greater than the 161,000 lbf calculated using the specified minimum tensile strength for two reasons. First, the load in the analysis is applied 3 in. closer to the hinge point in the end beam. This results in a higher strength. When this moment arm factor is accounted for, the strength calculated from the finite element analysis for a load centered in the corner post opening would be 216,000 lbf. This scaled value is 34 percent greater than the value calculated by hand. Most of this difference can be attributed to the higher actual tensile strength, 78,000 $lbf/in.^2$, which is 20 percent greater than the 65,000 $lbf/in.^2$ value assumed in the hand calculations. The rest of the difference is due to nonlinear effects not considered in the hand analysis such as the multiaxial deformation at the fracture location and the shortening of the moment arm with deformation.

Fracture is predicted to occur at a corner displacement of about 6.5 in. in both cases with a total energy absorption of about 110×10^3 ft-lbf (150 kJ). The conditions for the failure criterion given in Section 5 are as follows. The calculated principal stresses at the location of predicted failure, which is in the center of the plate element in front of the collision post hole, are: $\sigma_I = 152,000$ $lbf/in.^2$, $\sigma_2 = 53,000$ $lbf/in.^2$ and $\sigma_3 = 1,200$ $lbf/in.^2$. The quantities needed for the failure criterion given in Section 5 are then: $\sigma_m = 68,700$ $lbf/in.^2$ and $\sigma_e = 133,000$ $lbf/in.^2$. Then the predicted local effective plastic strain to failure is 0.68.

Figure 11 shows the deformed mesh at 5 in. of corner post displacement. The analysis also demonstrated that the fixture would not experience any significant plastic deformation or failure at connections. Load-crush predictions are compared to test results in the following test section.
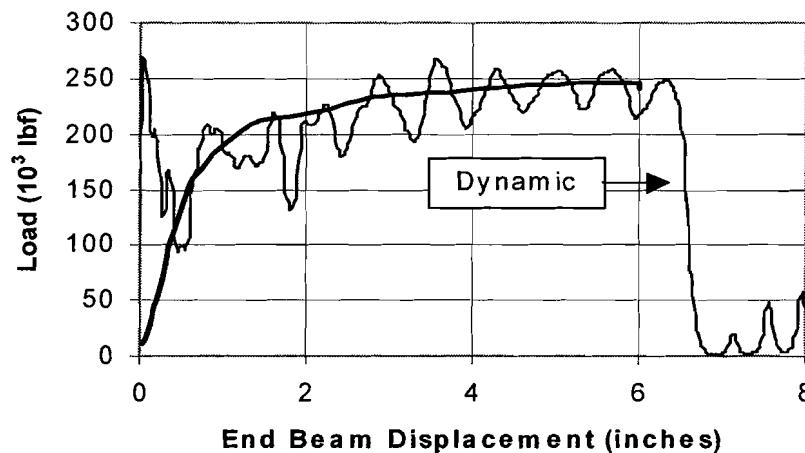
Figure 10. Predicted Load-Crush Responses for the Baseline End Beam Test Article Under Quasi-Static and Dynamic Loading

15
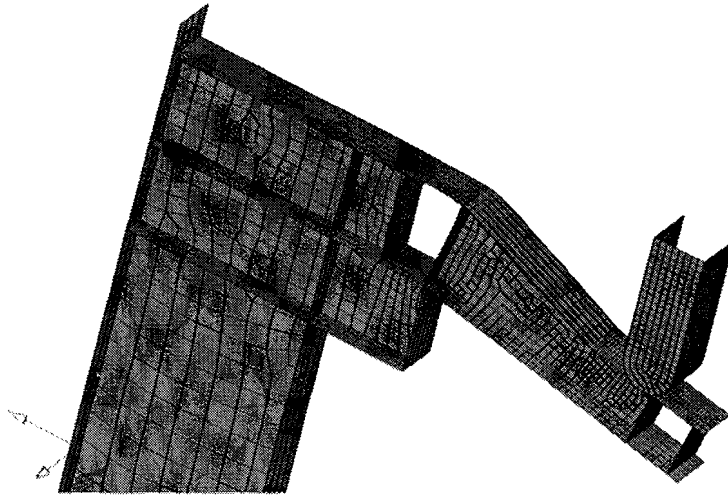
Figure 11. Deformed Mesh from the Quasi-Static Finite Element Analysis at the Location and Approximate Time of Fracture

5.2   MODIFIED TEST ARTICLE

The design of the supporting member for the modified test article was determined not only by the need to provide a higher peak strength but also to absorb energy through a regular folding pattern of deformation.

The cantilevered end beam and the supporting side sill column can be considered to act in parallel to a first approximation. The required strength of the column is then (using the minimum strength approach):

$$F_{req} = 400,000 - 161,000 = 239,000 \text{ lbf.}$$

The required cross-sectional area is assuming the column behaves as a compact element,

$$A_{min} = F_{req}/\sigma_{yield} = 239,000/50,000 = 4.78 \text{ in}^2.$$

The element chosen (Figure 5) has a cross-sectional area of 5.12 in.^{2} which gives a predicted total strength for the modified test article of 416,000 lbf.

A lateral support for the reinforcing side sill member was added to prevent buckling under plastic deformation.

The crush load for the reinforcing member can be estimated from the approximate equations provided in [6], which for a rectangular tube give,

$$F_m = 5.2Ct\sigma_{yield}(\frac{4t}{C})^{0.67}$$

where C = the outer dimension of the square tube and t = thickness. In the case where C = 7 in, t = 0.188 in., the predicted mean crush load is F_m = 77,000 lbf. This value was

16

confirmed with separate finite element analysis on the column element. This equation is approximate because the outer dimension of the square tube and the wall thickness change as the tube plastically deforms. In addition, the stresses in some regions of the cross-section are greater than the yield stress, and can approach or exceed the ultimate stress of the material.

The energy absorbed per unit crush for the column element is then, approximately,

$$E_{abs} = 77,000 \text{ ft-lbf/ft } (340 \text{ kJ/m}).$$

Higher energy absorption values could be obtained by selecting a column element with the same cross-sectional area but with a greater t/C ratio. The 7x7x0.188-in. member was selected to fit the dimensions of the test article and fixture.

The finite element analysis for the modified design was conducted using the same model as that used for the baseline geometry but modified to include the side sill supporting member. The model, after approximately 2 in. of simulated deformation, is shown in Figure 12; the predicted load-crush response is shown in Figure 13 compared to the dynamic response of the baseline end beam test article. The predicted peak load for the modified end beam is approximately 400,000 lbf. The corner displacement at which initial (end beam) failure is predicted was also 6 in. However, in this case, the analysis predicts that the supporting side sill member will still carry load and absorb energy. The total energy absorbed after 36 in. of crush is approximately 400,000 ft-lbf (540 kJ). At 36 in. of crush, the side sill element has crushed by approximately 63 percent of its initial length. It is estimated that the side sill could crush by approximately 40 in. – by approximately 70 percent of its initial length – before it would crush solid and the load it carries increases.
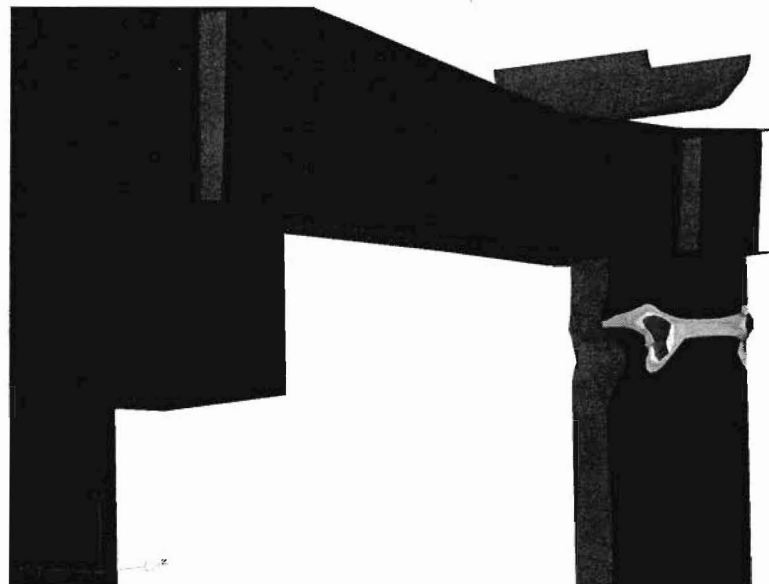
Figure 12.   Finite Element Model of Part of the Modified End Beam/Fixture After About Two Inches of Deformation
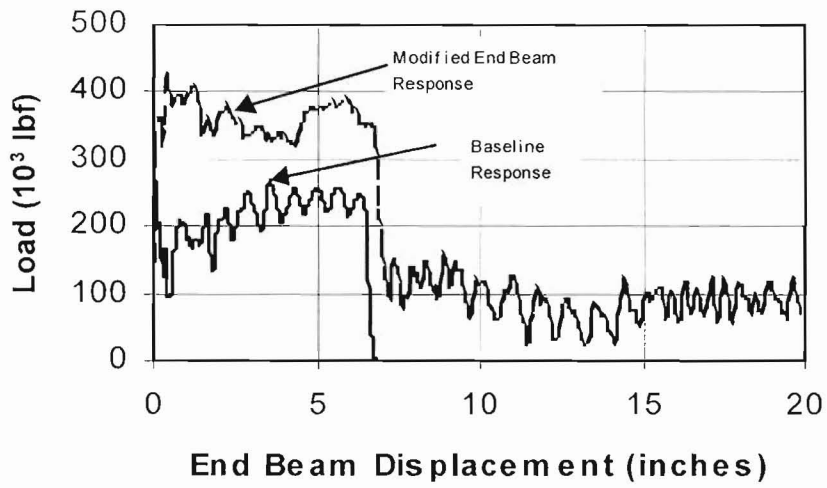
Figure 13. **Dynamic Load-Crush Response Predicted for the Baseline and Modified End Beam Test Article**

6. FABRICATION

Three baseline test articles were fabricated in accordance with engineering drawings; one of these was for use as the modified, higher-strength test article. Plate elements were flame cut and then welded together using the metal inert gas (MIG) process. A combination of full-penetration and fillet welds were used. In particular, the welds along the face of the end beam test article, which is in tension with the corner loading, were full-penetration welds. Welds were only visually inspected. This method of fabrication is typical of passenger rail car underframe construction.

Figures 14 shows a photograph of the completed baseline test article.

Figure 14.   Photograph of a Fabricated Baseline End Beam Test Article

All components were inspected upon receipt to ensure that they satisfied the engineering drawings.

Test articles were bolted to the test fixture via 16, 1.0 in. diameter x 8 tpi Grade 8 bolts. Hardened washers and Grade 8 nuts completed the interface. A torque of 890 ft-lbf per bolt was used.

7.   TESTING

The testing included quasi-static loading of one of the baseline test articles and dynamic, drop tower testing of a baseline and modified test article.

7.1   STRAIN GAGING

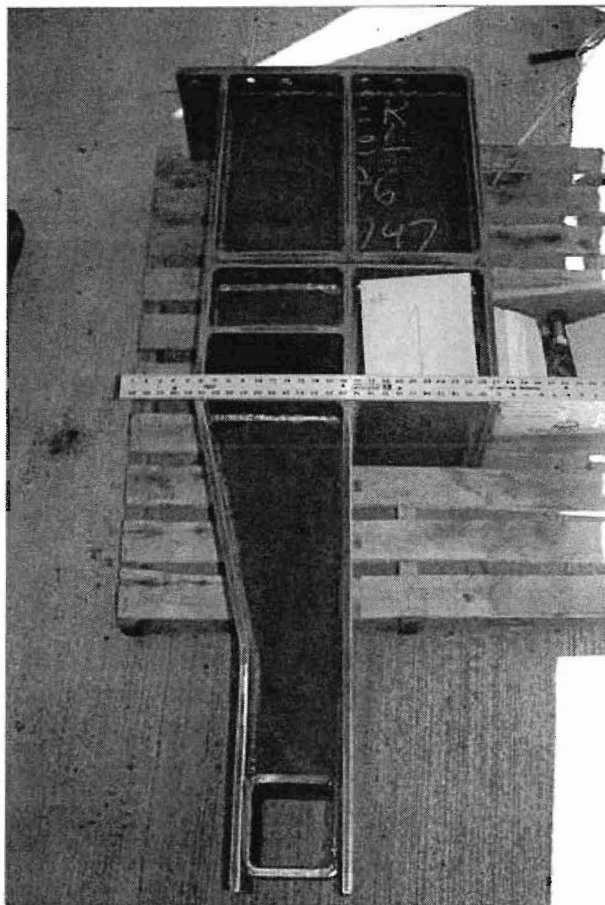Each test article was instrumented prior to testing with several strain gages as shown in Figure 15. The dimensions of Figure 15 are in inches. Six strain gages were applied to the baseline test articles. Two gages were applied to the fixture. Two gages were applied to the compression element of the modified end beam (represented by hidden lines in Figure 15), and two gages (9 and 10) were applied to the loading ram.
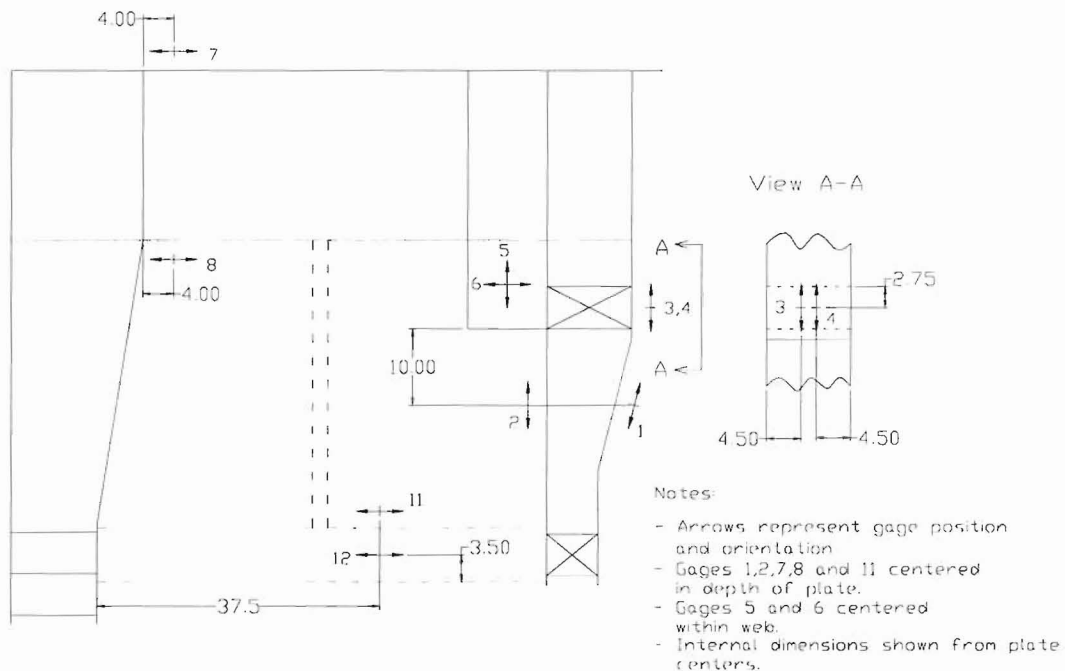
Figure 15. Strain Gage Placement on the Test Articles and Fixture

7.2   QUASI-STATIC TESTING

7.2.1   Procedure

The quasi-static testing was performed at the Transportation Sciences Center of Veridian/ Calspan in Buffalo, New York. The crush machine used consisted of a test bed, a fixed barrier, and a horizontally moving wall. The moving wall was driven by three, servo-controlled, hydraulic cylinders each rated to a maximum total compressive force of 150,000 lbf, and each in series with a load cell.

Figure 16 shows the baseline test article, the primary fixture and the loading fixture mounted in the quasi-static loading machine. The primary fixture was welded to the fixed wall and the loading fixture was welded to the moving wall and positioned to apply load in-line with the inner surface of the corner post lug.
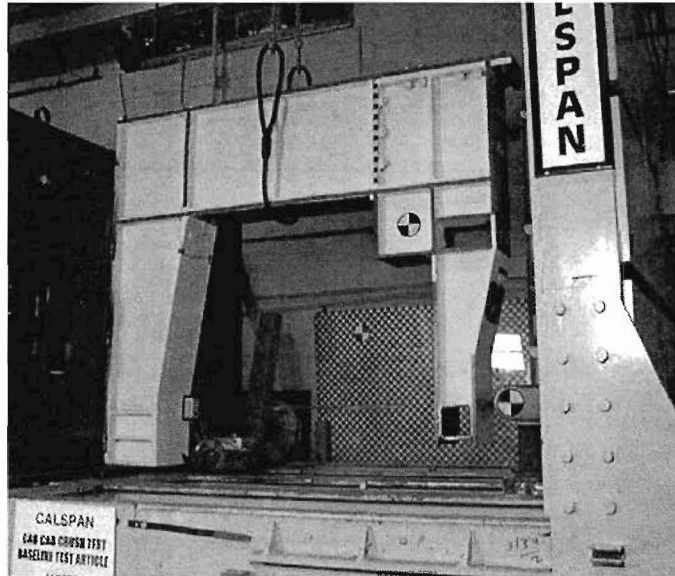
Figure 16. Quasi-Static Test Setup

In the course of conducting the test, an undesirable pitching of the moving wall was observed after approximately 1 in. of test article deformation. The test was then interrupted and the loading ram was supported vertically as shown in Figure 17 to prevent the pitch rotation. The vertical support rested on rollers that tracked on the crusher bed. This arrangement allows an accurate measurement of horizontal load, but does not permit the determination of the vertical load (as pictured) on the test article.
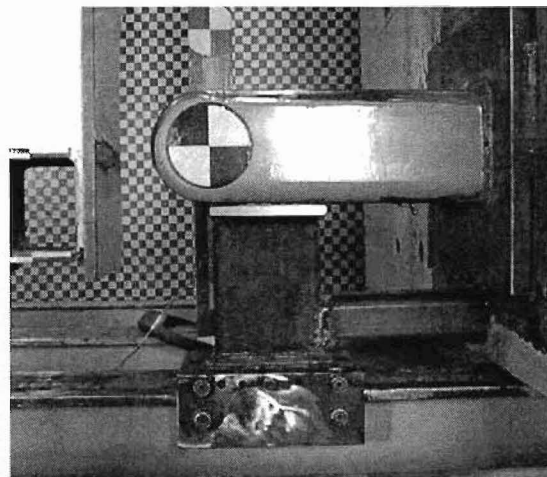
Figure 17.   The Vertical Support Used with the Quasi-Static Loading Fixture

Two displacement quantities were measured: the displacement of the moving wall relative to ground and the displacement of the end beam end relative to the primary test fixture.

The test set up and proceedings were recorded with both 35 mm and digital still photographs. Three video cameras recorded the actual test. One video camera framed the entire crush machine, fixture, and test article from the side. The second camera framed a side view of the test article. The third camera was mounted to the top of the moving wall and was focused on the front face of the collision post at the anticipated failure location.

The moving wall displacement rate was 1.25 in./minute. As mentioned above, the test was interrupted at a displacement of about 1 in. at which time the test article was unloaded, a vertical reinforcement was added to the loading fixture and the test was resumed to fracture.

7.2.2   Results

Figure 18 shows the measured load-displacement curve from the quasi-static test. The two sets of data from the two loading steps have been combined on this curve. The figure also includes the predictions from the finite element analysis for comparison.
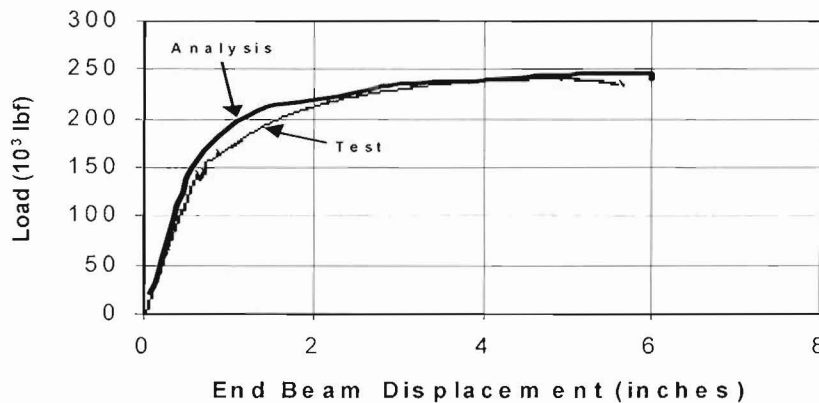
Figure 18.   Measured Load-Displacement Data from the Quasi-Static Baseline End Beam Test Compared to the Finite Element Model Predictions

Table 6 lists some of the key data obtained from the test. The measured ultimate load, as discussed previously, was over 240,000 lbf, 34 percent greater than the original design value. The energy absorbed was approximately 100,000 ft-lbf (130 kJ.)

Table 6. Key Data Obtained from the Quasi-Static Baseline End Beam Test

Ultimate Strength	242,000 lbf
Corner Displacement at Fracture	5.6 in.
Yield Strength	145,000 lbf
Deflection at Yield	0.6 in.
Elastic Stiffness	237,000 lbf/in.
Energy Absorbed	96,000 ft-lbf (130kJ)

Figures 19 and 20 show photographs of the test article after the test and, in particular, the location and form of fracture, which occurred in the plate element on the tension side of the collision post opening.

Figure 19. Photograph of the Baseline End Beam Test Article After Fracture in the Quasi-Static Test

Figure 20. Close-Up Photographs of the Fracture Location in the Quasi-Static, Baseline End Beam Test

Measurements were made after the test of the total stretch at the location of failure. These data showed that the average longitudinal strain at fracture in the plate element that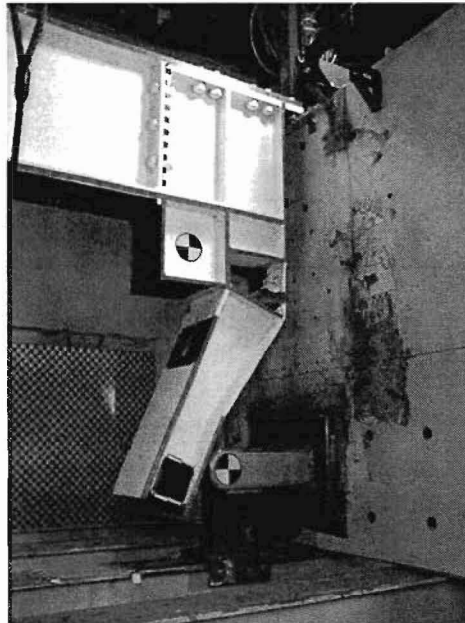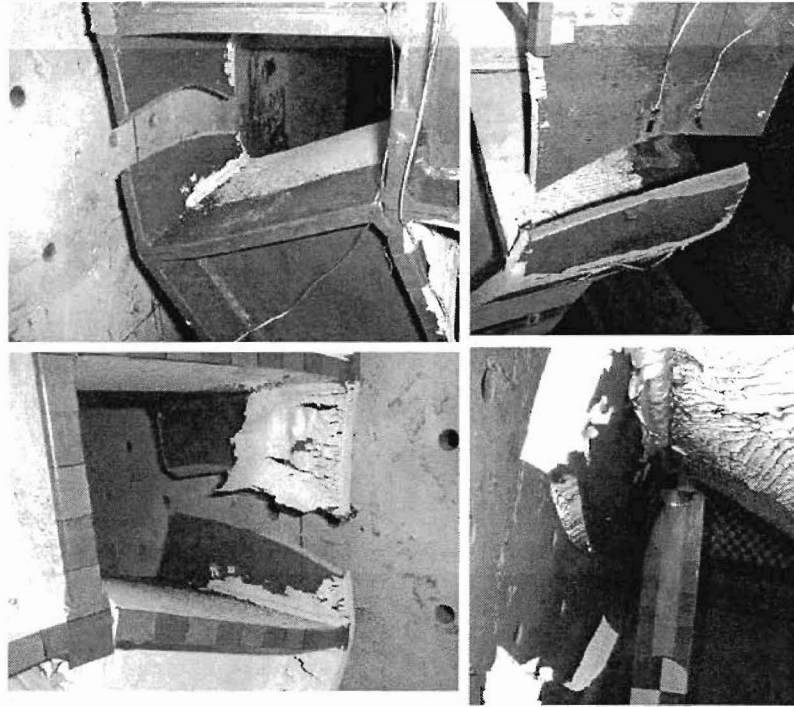 failed was approximately 0.28. This value is essentially equal to the elongation to failure in a tension test, 0.30, and much less than the true strain to fracture from the tension test, 1.05. The finite element analysis results corresponding to an end beam displacement of 5.6 in. give a predicted local effective plastic strain of 0.45, significantly less than the original predicted failure strain of 0.68. Nevertheless, predicted strength and energy absorption are within 10 percent of the measured values.

7.3   DYNAMIC TESTING

7.3.1   Procedure

Dynamic testing was conducted using a drop tower facility at Veridian/Calspan for which the maximum drop height, above the test article, was approximately 12 ft and whose total drop mass was 4,150 lbm. This equates to a total available energy of approximately 49,800 ft-lbf (68 kJ.) Because both the baseline and modified test articles were expected to absorb more energy than this, the need for multiple drops on each test article was also anticipated.

Figure 21 shows a photo of the drop tower with one of the test articles installed. The mass in the drop tower is guided to fall along a straight path by two adjacent parallel columns. In addition to the strain gage instruments discussed in Section 7.1, the dynamic tests

25

included two accelerometers mounted on the top of the mass (for use in deducing the load-time history on the test articles) and two high-speed cameras. A computerized data acquisition system was used to record all data except that from the cameras. Data collection was triggered by a contact switch at the impact point on the end beam.
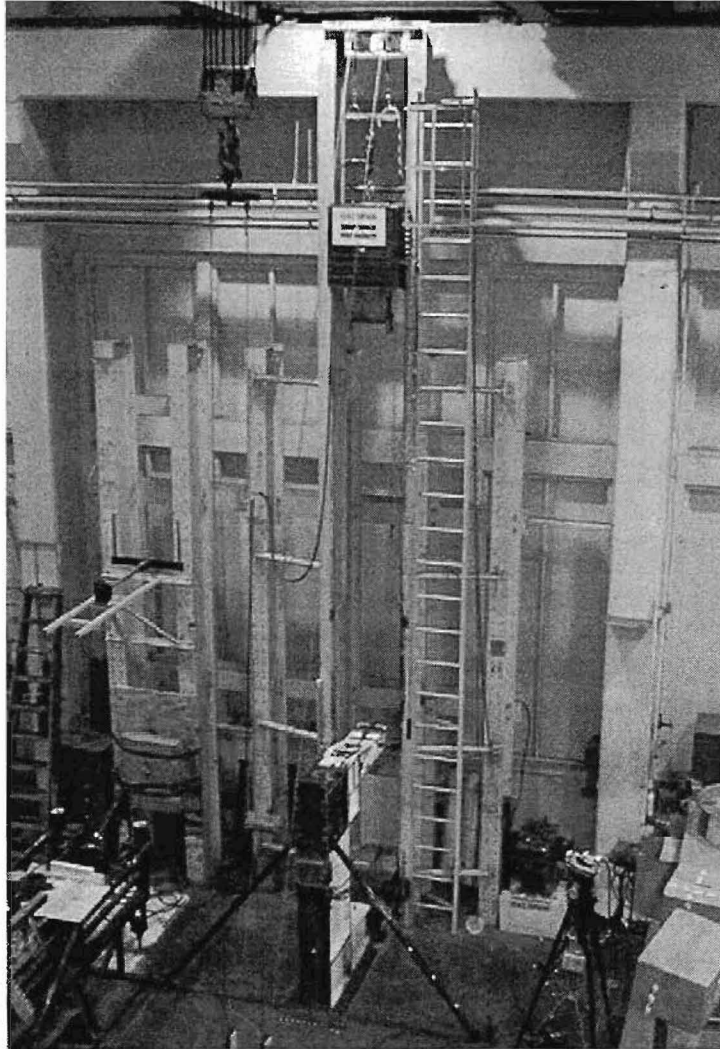
Figure 21. Photograph of the Drop Tower Facility with One of the Test Articles Installed

7.3.2 Baseline End Beam Test

The baseline end beam was subjected to two impacts from the drop tower for a total applied energy of about 100,000 ft-lbf (135 kJ). These impacts did not lead to fracture of the end beam.

During the second drop, a substantial amount of deformation occurred in the drop tower guide columns, evidently because of the lateral load induced from the bending of the end beam. Additionally, one of the drop mass guide column followers sheared its bolts

allowing the mass to rotate. Finally, the test fixture mounting bolts were loosened by the impact, providing evidence of yet another path for lost energy. As a result, the measured reaction force, based on the vertical component of acceleration, was much lower than that observed in the first drop. Because of the damage to the facilities, testing was ceased for the baseline article.

Figure 22 shows the measured load vs time for the first drop. The experimental load was calculated as the product of the average acceleration (from the two accelerometers) and the drop mass. Although there are isolated, short-duration dynamic peaks, it is clear that the peak strength is approximately 240,000 lbf as was also measured in the quasi-static test for this configuration. This and other key data are reported in Table 7.
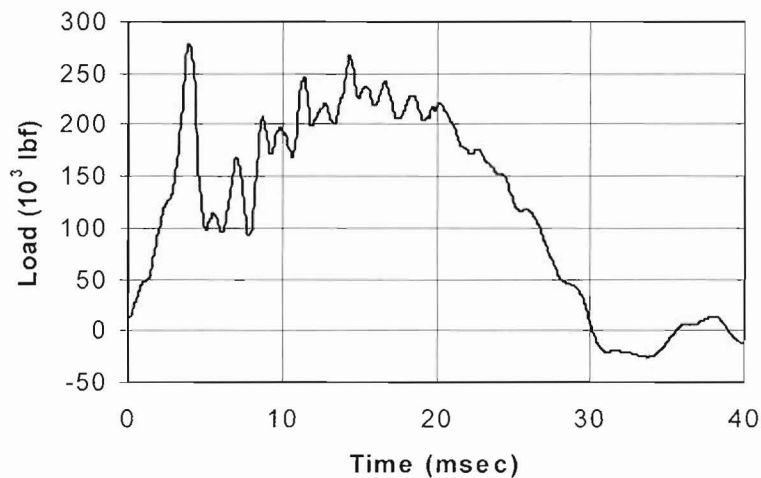
Figure 22.   Measured Load (from Accelerometer Data)-Time Data from Both Drops on the Baseline End Beam Test Article

Table 7.   Key Data Measured from the First Drop Test on the Baseline End Beam

Parameter	Drop 1
Approximate Peak Load	240,000 lbf
Permanent deflection of end beam end	1.8 in.
Avg. axial strain at the collision post opening plate	0.13
Drop Mass Rebound Height	20.4 in.

Rebound of the drop mass was observed in both impacts for this test article. Considering the rebound height, for the first drop the total energy delivered into plastic deformation of the test article/fixture assembly was actually about 42,700 ft-lbf (58 kJ).

Because of the facility's failures described, the energy absorbed by the test article in the second drop was significantly less than the first, and difficult to estimate. Substantially less energy than the 96,000 ft-lbf absorbed in the quasi-static test was converted to plastic deformation over the two drop tests. This explains why the article did not fracture during the test.

The first drop test provides the most useful results. The peak force of 240 kips echoes the quasi-static test. Additionally, excellent agreement between the finite element results and the experiment is demonstrated in Figure 23.
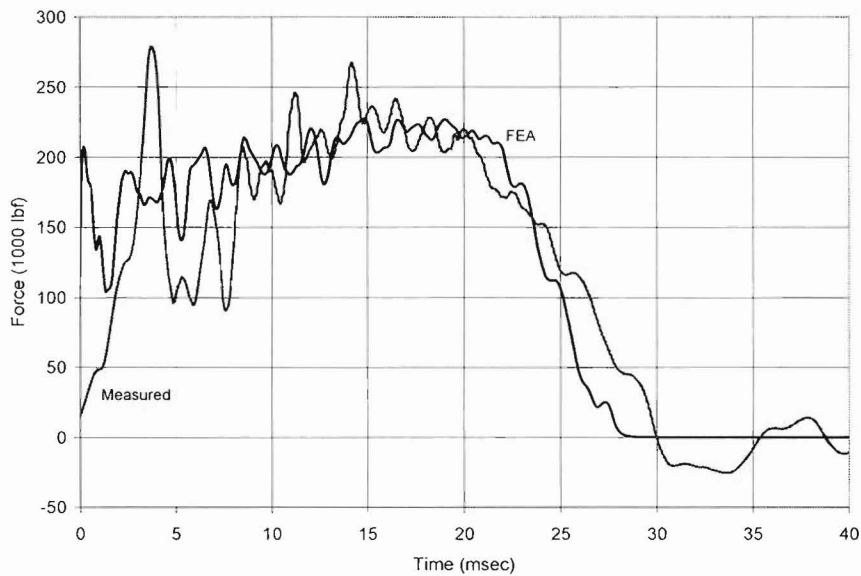

Figure 23.   Comparison of Measured and FEA-Predicted Load vs Time Data for the First Drop Tower Impact

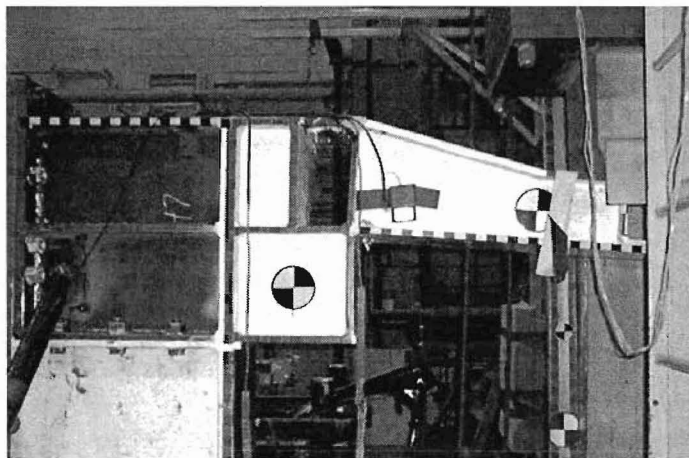Figure 24 shows a photograph of the baseline end beam test article after the first impact.

Figure 24.   Photograph of the Baseline End Beam Test Article after the First Drop Tower Impact

28

7.3.3 Modified End Beam Test

The modified end beam test article was also subjected to two impacts from the drop tower. It was felt that the two impacts would provide enough data to confirm the primary requirements set out for this design and to confirm the ability of the finite element analysis to simulate the entire crush process.

However, measurement system problems during both drops resulted in only a limited amount of data being available for the evaluation. In particular, the data obtained from both accelerometers are suspect, since there is a great difference between the individual accelerometer readings and there is also a physically unrealistic positive acceleration at the beginning of the test. The testing organization could not determine the cause of the anomalous form of the accelerometer data from these tests. In addition, the strain gage recording system did not function properly during the first drop, but appears to have functioned properly for the second drop.

Figure 25 shows the recorded data for the first impact for reference. The peak acceleration for one of the accelerometers is 150, which corresponds to a load of about 450,000 lbf. The peak acceleration from the other instrument is 400, which corresponds to a load of about 1,660,000 lbf, which is clearly not possible.
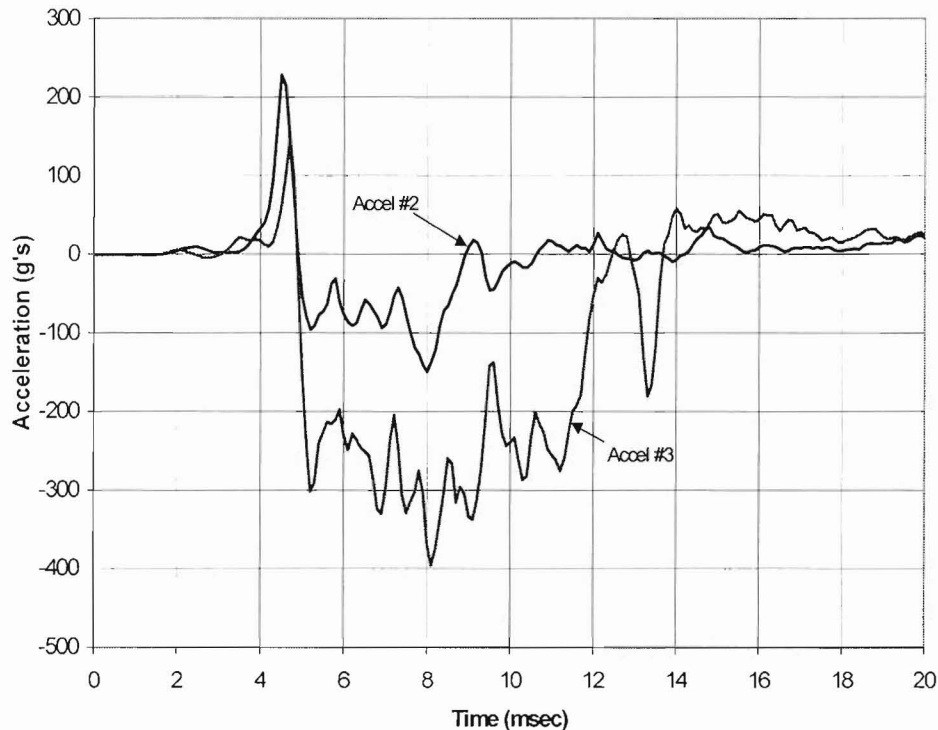

Figure 25. Recorded Accelerometer Data from the First Impact on the Modified End Beam Test Article

29

The only reliable data available from the first impact is a measurement of permanent displacement of the end beam. The value of this displacement for the two impacts on the modified end beam and some other data for the second drop are shown in Table 8.

Table 8. Some of the Key Data Measured in the Dynamic, Modified End Beam Tests

Parameter	First Drop	Second Drop
End beam permanent displacement	0.80 in.	1.71 in.
Peak strain in the end beam (gage 1)*	NA	1700×10^{-6}
Peak strain in the side sill column (gage 11)*	NA	1200×10^{-6}

* These values were taken at the same time increment.

Figure 26 shows the form of deformation at the top of the side sill element after the first drop. The folding type deformation desirable for energy-absorbing elements has been initiated.
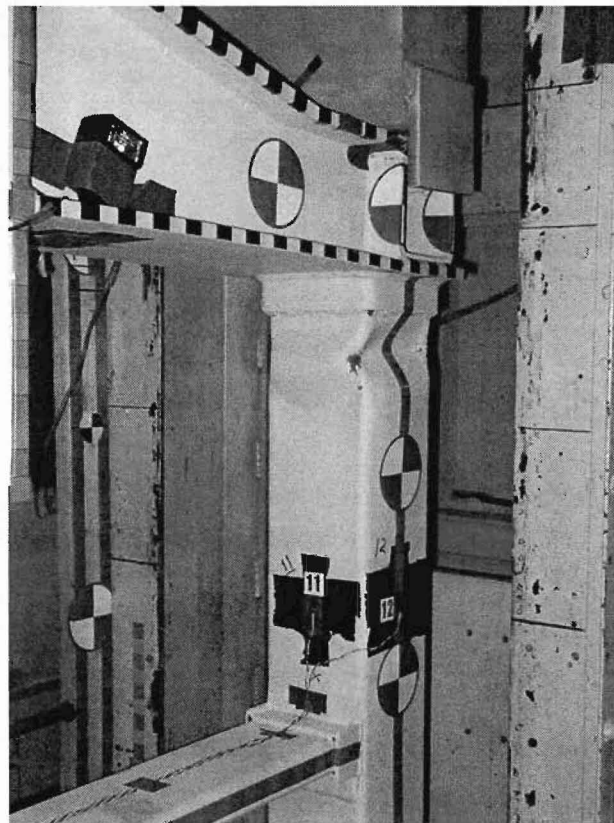

Figure 26. Photograph of the Modified End Beam at the Top of the Side Sill Element After the First Impact

The approach to estimating the ultimate strength for the modified end beam, which would have been exhibited for the first impact, is as follows:

1)   Estimate the experimental load-time history for the second impact, using the available elastic strain data and correlations between strain and load for the end beam elements.
2)   Modify the finite element analysis as needed to obtain agreement between the simulation and the available results, which are the end beam displacement data and the form of deformation for both impacts as well as the measured strains for the second impact.
3)   Use the predicted peak load from the analysis for the first impact as the measure of ultimate strength for the modified end beam test article.

The strain-time histories for strain gages located on the end beam and the side-sill column are shown in Figure 27, for the second impact. Both of these strain gages are located in regions that do not experience plastic deformation in the tests. The correlation between strain and load is made by assuming that the end beam and the side-sill element act as parallel springs so that the force in each can be added. The strain-load correlation in the end beam is made by treating the end beam as a simple cantilever beam. The side-sill element acts as a simple column in compression.
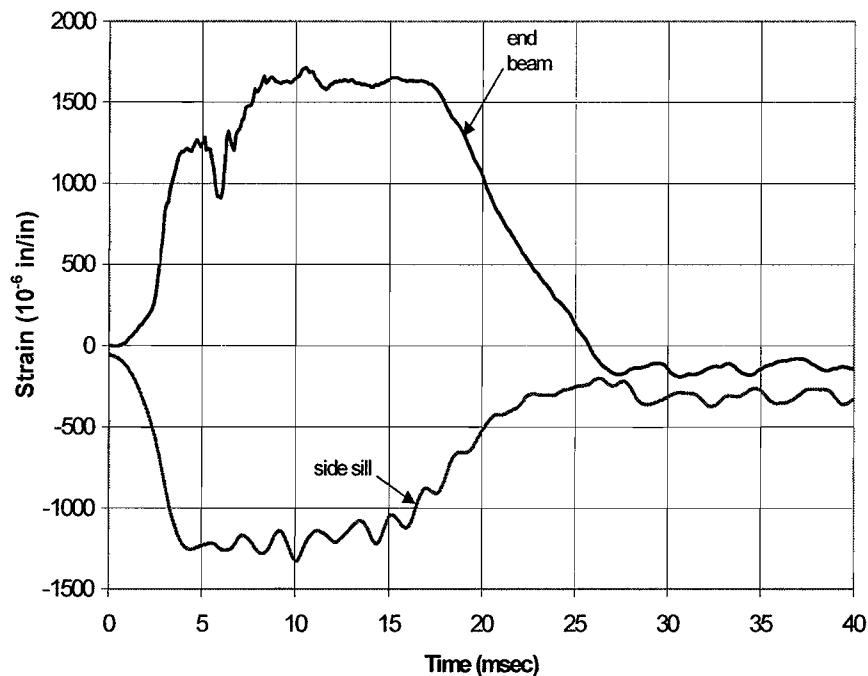

Figure 27.   Measured Strain-Time Histories for the Second Impact on the Modified End Beam Test Article

Figure 28 shows the strain-derived load vs. time plot for the second impact in comparison to the finite element analysis prediction, and Table 9 compares the measured and finite

31

element analysis predictions for the permanent displacement of the end beam end for the two impacts. These represent the optimized predictions. The finite element analysis used for these predictions includes all the assumptions previously described. (The only change that was necessary to obtain agreement between the strain-derived load and measured displacements and the finite element predictions was to use material strength values for the side sill element that were the same as those used for the A572 Grade B steel.)
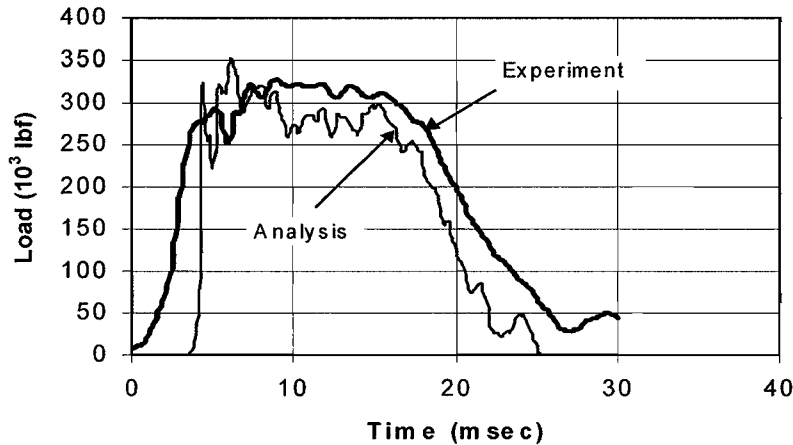

Figure 28. Load-Time History for Second Impact of Modified End Beam, Derived from Strain-Time Histories for End Beam and Side Sill Structural Elements with Comparison to Finite Element Predictions

Table 9. Comparison of Measured and Predicted Load Displacements for the Modified End Beam Test Article

Impact	Measured Permanent Displacement (inches)	Permanent Displacement Predicted from the Finite Element Analysis (inches)
1	0.80	0.96
2	1.71	2.48

Finally, Figure 29 shows the load-time response predicted by the optimized finite element analysis for the first impact. The predicted peak load is just over 400,000 lbf, which matches the design goal. Figure 30 shows the predicted energy absorbed vs. load displacement for a total displacement of 20 in. (Figure 13 showed the predicted load-crush response for a deformation of 20 in.) A total energy absorption of 300,000 ft-lbf (410 kJ) is predicted at 20 in. of crush and, through extrapolation, it is predicted that 450,000 ft-lbf (610 kJ) would be absorbed after 36 in. of crush.
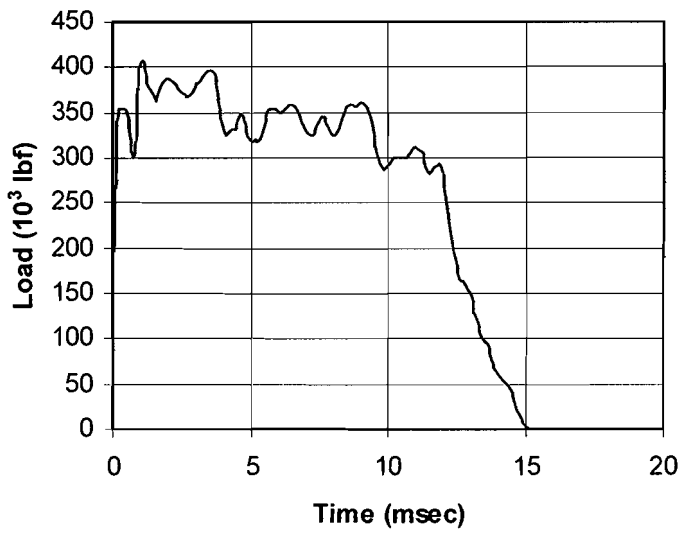
32

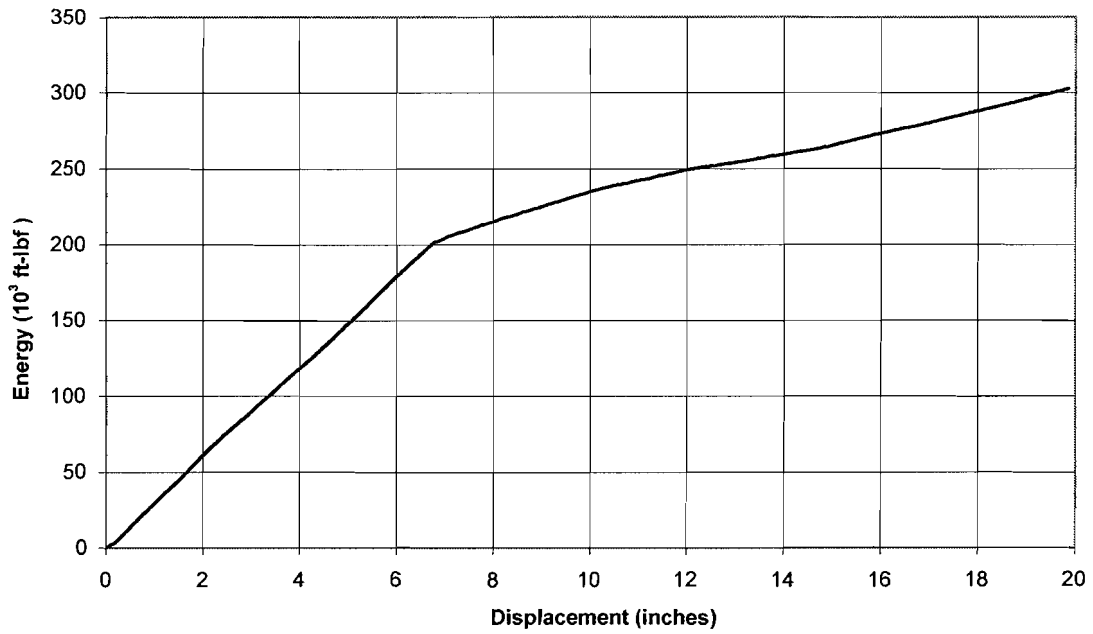**Figure 29. Overall Predicted Load-Time Response of the Modified End Beam Test Article**

Figure 30. Predicted Absorbed Energy vs. Load Point Displacement for the Modified End Beam Test Article

8. DISCUSSION

The results from this program have demonstrated a number of key points. The conventional techniques used for ultimate strength design in rail vehicles can lead to very conservative results relative to the strength goals. The baseline end beam was designed to have an ultimate strength of 150,000 lbf with some margin. The measured value was 240,000 lbf. This added strength comes from material properties that were greater than the material minimum requirements and from material and geometric nonlinearities that were not considered in the hand calculations. Many of the rail vehicles currently on the road and designed to the 150,000 lbf strength value have substantially higher strengths and energy absorption potential. Such a difference has been found for other rail vehicle structural components such as the collision posts and anticlimbers on freight locomotives [7].

It may be possible to cite the disparity between the design goal and actual strength as an indication that the corner structures built to current standards provide more protection than has been calculated as possible in previous studies [4,5]. However, this study demonstrates how the use of accurate material property data and finite element analysis techniques can enable a vehicle designer to potentially save weight and cost in meeting various structural requirements. Since the use of finite element analysis for ultimate strength design is becoming more widespread, the differences between design and actual strengths can be expected to become smaller in the future. Therefore, the minimum crashworthiness requirements must be specified accurately.

This study also has shown how the addition of a relatively simple longitudinal member can substantially increase the strength and energy absorption capability of a cab car corner. In this study, this longitudinal member had a total weight of just 80 lbf.

The strength of the corner structure was increased to over 400,000 lbf and the energy absorption in one foot of crush was increased from 100,000 ft-lbf (135 kJ) to 250,000 ft-lbf (340 kJ). If the baseline design had just met the 150,000 lbf ultimate strength requirement the baseline energy absorption would have been approximately 63,000 ft-lbf (85 kJ) and the increase in energy absorption provided by the modified design would have been a factor of four.

The original hand calculations were based on the assumption that the peak strengths of the end beam cantilever member and the longitudinal column would be achieved simultaneously. However, this did not occur. Figure 18 shows that the peak strength of the cantilever element is achieved only after about 5 in. of deformation, close to the point of fracture. On the other hand, the peak load in the compression element is achieved at much smaller displacements, corresponding to the beginning of yielding of the column before the folding-type deformation initiates. Figure 31 shows the computed contribution of only the compression element obtained by subtracting the load at a particular displacement for the baseline end beam from the total load at the same displacement for the modified end beam test article. The peak strength of the compression element, which

is equal to about 260,000 lbf, occurs at a displacement of about 0.5 in., after which the load levels off to an average crush load of about 80,000 lbf, as predicted by hand calculations. Since the strength of the cantilever end beam element at 0.5 in., Figure 18, is about 150,000 lbf, a total peak strength for the modified end beam of approximately 400,000 lbf is obtained.
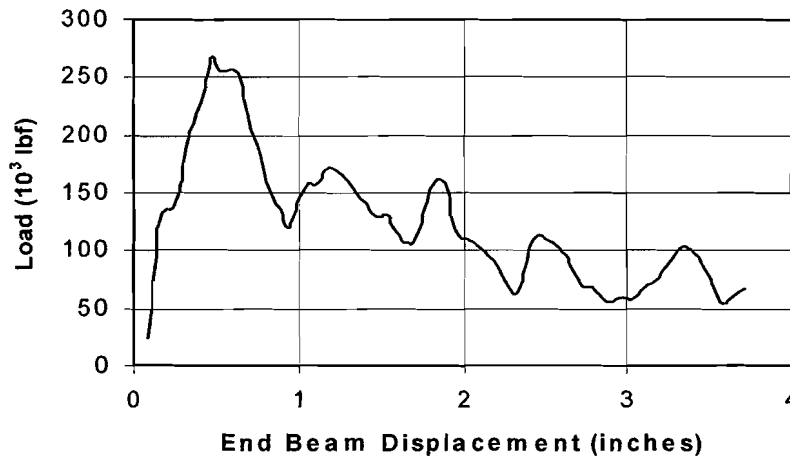

Figure 31.   Computed Contribution of the Side Sill Compression Element in the Modified End Beam Test Article

Therefore, to obtain an even greater strength of the corner element, the cross-sectional area, or the yield strength of the side sill element would need to be increased. For example, an increase in cross-sectional area to 7.5 in.^{2} for the same yield strength of 50,000 lbf/in.^{2} would increase the total modified end beam strength to about 550,000 lbf.

The other change that could be made to absorb more energy is to lower the C/t ratio for the side sill element while maintaining approximately the same cross-sectional area. For example, a 5x5x5/16-in. steel square tube with a yield strength of 50,000 lbf/in^2 provides a slightly larger weight per unit length than the 7x7x3/16-in. tube used in these tests, but its average crush load is about 160,000 lbf, compared to 80,000 lbf. In the rail vehicle, the side sill supporting structure would also have to be designed to carry these higher crush loads.

Each side sill element weighs approximately 80 lbs. Adding four such elements to a car would potentially increase its weights by 320 lbs., an increase in car weight of approximately 0.3 percent. A side sill element with a cross-sectional area of 7.5 in^2 would weigh approximately 120 lbs, and four such elements would potentially increase the weight of the car by approximately 0.5 percent.

In summary, this experimental and analysis study has demonstrated that the corners of cab cars can be modified to provide greater strength and energy absorption without substantial weight penalty. The study has also shown that nonlinear finite element analysis used with accurate material properties provides a very effective tool for

36

determining the ultimate strength and energy absorption properties of rail vehicle structures under collision type loading.

REFERENCES

1. National Transportation Safety Board, "Railroad Accident Report: Near Head-on Collision and Derailment of Two New Jersey Transit Commuter Trains Near Seacaucus, New Jersey February 9, 1996," PB97-916301, NTSB-RAR-97-01 (March 25, 1997).

2. National Transportation Safety Board, "Collision and Derailment of Maryland Rail Commuter MARC Train 286 and National Railroad Passenger Corporation AMTRAK Train 29 Near Silver Spring, Maryland on February 16, 1996," PB97-916302, NTSB-RAR-97-02 (June 17, 1997).

3. National Transportation Safety Board, "Collision Between Northern Indiana Commuter Transportation District Eastbound Train 7 and Westbound Train 12 Near Gary, Indiana on January 18, 1993," PB93-916304, NTSB-RAR-93-03 (December 7, 1993).

4. Tyrell, D.C., K.J. Severson, R.A. Mayville, R.G. Stringfellow, S. Berry, and A.B. Perlman, *Evaluation of Cab Car Crashworthiness Design Modifications*, in Proceedings of the 1997 ASME/IEEE Joint Railroad Conference, March 18-20, 1997 Boston, Massachusetts, 49-58.

5. Stringfellow, R.G., R.A. Mayville, and R.J. Rancatore, *A Numerical Evaluation of Protection Strategies for Railroad Cab Car Crashworthiness,* American Society of Mechanical Engineers, AMD Vol., 237/BED Vol., 45, 1999.

6. Structural Impact, N. Jones (Cambridge, UK; Cambridge University Press) 1989.

7. Mayville, R.A., et al., *Locomotive Crashworthiness Research, Volumes 1-5,* Department of Transportation, DOT/FRA/ORD-95/08.1, 1995.